Fabrication and Evaluation of PVA-NYS-THY Nanofiber Scaffolds as Antifungal Agents Against Fluconazole-Resistant *Candida glabrata*

Romina Ahmadian [1], Mohaddeseh larypoor [2*], Mansour Bayat [3]

1. Department of Biology, Faculty of Biological Sciences, Islamic Azad University, Tehran North Branch, Tehran, Iran. ORCID: 0009-0001-7896-8383

2. Department of Biology, Faculty of Biological Sciences, Islamic Azad University, Tehran North Branch, Tehran, Iran, m.larypoor@iau-tnb.ac.ir, ORCID:0000-0002-2003-8343

3. Department of Veterinary Pathobiology, S.R.C., Islamic Azad University, Tehran, Iran

ORCID: 0000-0001-8329-4283

Corresponding Author:

Mohaddeseh larypoor, m.larypoor@iau-tnb.ac.ir, ORCID:0000-0002-2003-8343, Phone: +98 21 84473528

Abstract

The emergence of fluconazole-resistant *Candida glabrata* poses a significant challenge in antifungal therapy, necessitating alternative treatment strategies. *C. glabrata*, an opportunistic yeast, exhibits increasing resistance to common antifungals like fluconazole, often through efflux pump overexpression, leading to compromised treatment efficacy, higher mortality, prolonged hospital stays, and increased healthcare costs. This study focused on fabricating and evaluating polyvinyl alcohol-nystatin-thymol (PVA-NYS-THY) nanofibrous scaffolds as a novel antifungal approach against fluconazole-resistant *C. glabrata*. Clinical isolates were identified and assessed for resistance using culture methods, molecular assays, and antifungal susceptibility testing. PVA-NYS-THY nanofibers, produced via electrospinning, exhibited uniform fibers with an average diameter of ~100 nm (confirmed by scanning electron microscopy). Fourier transform infrared spectroscopy confirmed successful incorporation of functional groups. Real-time PCR evaluated the nanofibers' effect on secreted aspartyl proteinases (SAP) and agglutinin-like sequence (ALS) gene expression. Scaffold release kinetics were characterized, and antifungal efficacy was determined using minimum inhibitory concentration (MIC) assays. PVA-NYS-THY scaffolds showed favorable release profiles and significantly downregulated ALS and SAP gene expression. MIC values for PVA-NYS-THY, PVA-NYS, and PVA-THY were 7.81, 15.62, and 62.5 µg/mL, respectively, demonstrating superior antifungal activity of the PVA-NYS-THY

formulation. These findings suggest PVA-NYS-THY nanofibrous scaffolds offer a promising therapy for fluconazole-resistant *C. glabrata*, providing a novel solution to overcome current therapeutic limitations.

Keywords: Antifungal activity; Biocompatible materials; Drug delivery; Nystatin; Thymol

1. Introduction

Candida glabrata, an opportunistic yeast within the *Candida* genus, presents a growing threat to human health, particularly due to increasing antifungal resistance. Candidiasis, infections caused by *Candida* species, can manifest in various anatomical locations, including the oral cavity, esophagus, vagina, urinary tract, skin, and bloodstream (1). Immunocompromised individuals are particularly susceptible to severe candidiasis (2). Effective management is challenged by limited antifungal drugs and the rise of drug resistance, especially in *C. glabrata*, which frequently exhibits azole resistance due to efflux pump overexpression or *ERG11* gene mutations (3). This resistance leads to high mortality, prolonged hospital stays, and increased healthcare costs (4), necessitating innovative therapeutic strategies.

Several approaches have been explored to combat fungal infections, including conventional antifungal drugs (e.g., azoles, polyenes, echinocandins) and various drug delivery systems. Traditional antifungal therapies often suffer from limitations such as poor solubility, instability, limited bioavailability, and systemic toxicity (5). For instance, topical formulations have limited penetration into deeper tissues, while oral and intravenous administrations can cause adverse side effects. Furthermore, the emergence of drug resistance significantly reduces the efficacy of these conventional treatments. This highlights the need for improved drug delivery systems.

Nanomaterials, particularly nanofibers, offer a promising alternative by addressing these limitations. These ultrafine fibers (diameter <1000 nm) possess a high surface area-to-volume ratio, tunable porosity, flexibility, and mechanical strength, enabling improved drug delivery (5). Encapsulating antifungal drugs within nanofibers can enhance drug solubility, stability, and bioavailability while reducing non-specific toxicity. Controlled release from nanofibers ensures sustained drug delivery to the infection site, minimizing systemic toxicity and maintaining therapeutic concentrations at the target site, potentially reducing administration frequency. Various methods exist for nanofiber

production, including drawing, template synthesis, self-assembly, and electrospinning (6). Electrospinning, chosen for this study, offers several advantages over other methods: it is relatively simple, versatile (allowing the use of various polymers and drugs), scalable for large-scale production, and cost-effective (6). This justifies our choice of electrospinning for this research.

This study develops and evaluates a novel antifungal formulation using electrospun nanofibers loaded with nystatin and thymol (PVA-NYS-THY) to combat *C. glabrata* infections. Nystatin, a polyene antifungal effective against *Candida* species, targets ergosterol in fungal membranes, disrupting membrane integrity and causing cell death (7). However, its clinical use is limited by poor solubility, instability, toxicity, and bioavailability (8). Encapsulation within nanofibers aims to overcome these limitations. Thymol, a natural phenolic monoterpene with antifungal properties, disrupts membrane integrity, binds to ergosterol, and increases membrane permeability, facilitating antifungal entry (9). Combining nystatin and thymol is hypothesized to produce a synergistic effect against *C. glabrata*, potentially reducing the required nystatin dose and minimizing toxicity (10). This study specifically examines the impact of PVA-NYS-THY nanofibers on the expression of key virulence genes, *SAP* and *ALS*, in *C. glabrata*. SAP enzymes facilitate tissue invasion and immune evasion, while ALS glycoproteins mediate adhesion and biofilm formation (11). We hypothesize that PVA-NYS-THY nanofibers will modulate these genes, reducing *C. glabrata* virulence. Our goal is to assess PVA-NYS-THY nanofibers as an innovative antifungal formulation to enhance nystatin efficacy against this challenging pathogen.

2. Materials and methods

2.1. Sample collection and preparation

Oral and vaginal swabs were collected from 100 patients with suspected candidiasis (from October 2023 to March 2024). Samples were cultured on *Candida* chrome agar and incubated at 30°C for 72 hours. Yeast colonies were initially identified based on morphological and biochemical characteristics. Twelve *C. glabrata* isolates were selected for further molecular characterization and antifungal testing. This study was approved by the Research Ethics Committee of Islamic Azad University (RECIAU no: 1401.0445), and all participants provided written informed consent, adhering to the Declaration of Helsinki.

2.2. Molecular Confirmation

Genomic DNA was extracted from the 12 selected isolates using the phenol-chloroform method. The 18S rRNA gene was amplified by PCR using specific primers (FW: AGCTGGTTGATTCTGCCAG, RV: TGATCCTCCYGCAAGTTCAC), purified, and sequenced (Pishgam Biotechnology Company). Sequence alignment (ClustalW) and phylogenetic analysis (MEGA7) confirmed the isolates as *C. glabrata*. PCR was also used to detect *ALS* and *SAP* gene families using specific primers.

2.3. Materials and Nanofiber Preparation

Thymol ($C_{10}H_{14}O$, 150.22 g/mol, EC 201-944-8) and nystatin (Sigma-Aldrich) met analytical standards (Ph. Eur., BP, NF, USP). Stock solutions (10 mg/mL) were prepared in dimethyl sulfoxide (DMSO). The final DMSO concentration in experiments was kept below 1% (v/v). Polyvinyl alcohol (PVA, 89,000–98,000 g/mol) was dissolved in distilled water (10% w/v) and stirred at 80°C for 4 hours. Three nanofiber formulations were prepared via electrospinning (Nanospinner NS24, Inovenso, Turkey): PVA-nystatin (1% w/v), PVA-thymol (1% w/v), and PVA-nystatin-thymol (0.5% w/v each). Electrospinning parameters were optimized as follows: flow rate (1 mL/h), voltage (15 kV), needle-collector distance (15 cm), 25°C, and 40% humidity. Nanofibers were collected on aluminum foil and dried in a vacuum oven at 40°C for 24 hours.

2.4. Nanofiber Characterization and Drug Release:

Nanofiber morphology (diameter) was assessed using scanning electron microscopy (SEM, JSM-6390LV, JEOL, Japan) after gold coating. ImageJ software was used for diameter analysis. Fourier-transform infrared (FTIR) spectroscopy confirmed the presence of nystatin and thymol within the PVA matrix. Drug release kinetics were studied using a dialysis method (12). Nanofibers containing 10 mg of drug were placed in dialysis bags (12,000-14,000 Da cutoff) and immersed in 50 mL phosphate-buffered saline (PBS, pH 7.4) with 0.5% Tween 80. The bags were incubated at 37°C with agitation (100 rpm). At predetermined intervals, 1 mL aliquots were sampled and replaced with fresh PBS. Released drug concentrations were quantified using high-performance liquid chromatography (HPLC).

2.5. Antifungal Susceptibility Testing

Antifungal activity was assessed against *Candida albicans* ATCC 10231 and clinical *C. glabrata* isolates using two methods: a modified agar diffusion assay and broth microdilution for MIC/MFC determination.

2.5.1. Agar Diffusion Assay

Microbial suspensions were prepared in Mueller-Hinton Broth (MHB), incubated at 30°C for 18-24 hours, and adjusted to a 0.5 McFarland standard (approximately 1-5 x 10^6 CFU/mL) (CLSI M27, 2022). A 1:100 dilution (approximately 1-5 x 10^4 CFU/mL) was used to enhance visualization of inhibition zones. Six-millimeter nanofiber discs were placed on Mueller-Hinton Agar (MHA) plates inoculated with the fungal suspensions using a sterile swab to create a confluent lawn. Plates were incubated at 30°C for 24-48 hours. Inhibition zone diameters were measured using a digital caliper. All tests were performed in triplicate (n=3), and results are presented as means ± SD.

2.5.2. Broth Microdilution Assay (MIC/MFC)

MIC and MFC values for nystatin, thymol, and the PVA-NYS-THY combination were determined using the broth microdilution method according to CLSI M27 (2022) and adapted for testing of nanofibers. Serial twofold dilutions of each agent were prepared in 96-well microtiter plates using 3-(N-morpholino) propanesulfonic acid (MOPS)-buffered RPMI 1640 medium. Tested concentrations were: nystatin (0.039–125 µg/mL), thymol (0.625–2000 µg/mL), and PVA (0.078–25 mg/mL). DMSO (used as a solvent for thymol) was kept below 1% (v/v). A 100 µL inoculum (prepared as in Section 2.5.1) was added to 100 µL of drug solution per well (200 µL final volume). Plates were incubated at 30°C for 24-48 hours. MIC was determined as the lowest concentration inhibiting visible growth. For MFC, 10 µL from no-growth wells (at or above the MIC) was subcultured onto Sabouraud dextrose agar (SDA) and incubated at 30°C for 48 hours. MFC was defined as the lowest concentration with no growth on SDA.

2.6. Fractional inhibitory concentration index calculation

The fractional inhibitory concentration index (FICI) was calculated to evaluate the interactions between the antifungal agents in the combinations. The FICI was obtained by adding the FIC values of each drug in the combination, where FICI = MIC of the drug in combination / MIC of the drug alone. The FICI was interpreted as follows: ≤0.5, synergism; >0.5-4, indifference; >4, antagonism.

$$\mathrm{FICI} = \frac{\mathrm{MIC_A\,combination}}{\mathrm{MIC_A\,alone}} + \frac{\mathrm{MIC_B\,combination}}{\mathrm{MIC_B\,alone}}$$

where MIC_A combination and MIC_B combination are the minimum inhibitory concentrations (MICs) of drug A and drug B when used in combination, and MIC_A alone and MIC_B alone are the MICs of drug A and drug B when used alone.

2.7. Real Time PCR

Real-time PCR assessed the effect of nystatin- and thymol-incorporated PVA nanofibers on *SAP* and *ALS* gene expression in *C. glabrata* isolates. Isolates were treated with sub-MIC concentrations of nanofibers. Total RNA was extracted (RNeasy Mini Kit, Qiagen), and cDNA was synthesized from 1 µg RNA (RevertAid First Strand cDNA Synthesis Kit, Thermo Fisher Scientific). Primers targeting *SAP* and *ALS* (Alves et al., 2014) (13) (primer sequences in Table 1) and the *ACT1* housekeeping gene were used. qPCR (20 µL) used SYBR Green Master Mix (Applied Biosystems), 10 pmol/µL primers, 2 µL cDNA, and nuclease-free water. Cycling conditions: 95°C for 10 min; 40 cycles of 95°C for 15 s, 60°C for 30 s, and 72°C for 30 s. Relative gene expression was calculated using the $2^{-\Delta\Delta Ct}$ method (StepOne Software v2.3, Applied Biosystems).

Table 1. Primers sequence employed in qRT-PCR analyses (20)

Primer	Sequence	Tm (C°)	Amplicon size (bp)
***ALS*-F**	CTGGACCACCAGGAAACACT	59.53	226
***ALS*-R**	GGTGGAGCGGTGACAGTAGT	61.53	
***SAP*-F**	ACCGTTGGATTTGGTGGTGTTT	61.21	218
***SAP*-R**	ATTATTTGTCCCGTGGCAGCAT	60.95	
ACT-F	TTGCCACACGCTATTTTGAG	55	167
ACT-R	ACCATCTGGCAATTCGTAGG	55	

2.8. Statistical Analysis

All experiments were performed in triplicate (n=3), and data are presented as means ± standard deviation (SD). The normality of data distribution was assessed using the Shapiro-Wilk test. For comparisons between multiple groups, a one-way analysis of variance (ANOVA) was performed. If the ANOVA indicated statistically significant differences

($p \leq 0.05$), Tukey's Honestly Significant Difference (HSD) post hoc test was used for pairwise comparisons to determine which specific groups differed significantly from each other. These analyses were performed using GraphPad Prism (version 9.0, GraphPad Software, San Diego, CA, USA).

3. Results

3.1. Clinical Isolation, Molecular Characterization, and Antifungal Susceptibility of *Candida glabrata*

This study characterized 13 *C. glabrata* isolates (13% prevalence, 26% of all Candida species) from 100 clinical samples. Oral swabs were the primary source (69%), followed by vaginal swabs (23%) and urine (8%). Infected patients (mean age 45.2 years) were predominantly female (53.85%), with most reporting no tobacco or alcohol use (84.62%). ICU admission (30.77%) and central venous catheter presence (69.23%) were common risk factors, while vulvovaginal candidiasis (VVC) (23.08%), including recurrent VVC (23.08%), was the most frequent diagnosis (Supplementary Table S1). Molecular identification using *18S rRNA* gene sequencing confirmed *C. glabrata* in 8 of 11 suspected isolates, exhibiting a 1500 bp PCR product and clustering phylogenetically with reference strains (Supplementary Figure 1). The remaining three isolates were identified as other Candida species. Virulence genes *ALS* and *SAP* were detected in all confirmed *C. glabrata* isolates. Morphological and biochemical analyses (Supplementary Figure 2) corroborated these findings. Importantly, all *C. glabrata* isolates exhibited fluconazole resistance but susceptibility or semi-susceptibility to amphotericin B, nystatin, and ketoconazole (Supplementary Figure 3).

3.2. Characterization of PVA-Nystatin-Thymol nanofibers

Optimized PVA nanofibers containing nystatin and thymol (3:7 ratios to PVA) yielded smooth, uniform, knot-free nanofibers, as observed visually and confirmed by Scanning electron microscopy (SEM) (Figure 1), showing an average diameter of ~100 nm. FT-IR spectroscopy (Figure 2) revealed characteristic peaks for PVA, nystatin, and thymol, including O-H, N-H, C-H, C=O, C=C, C-N, and C-O groups. Crucially, peak shifts and splitting, such as the splitting of nystatin's C=O stretch (1728 cm^{-1} to 1724 cm^{-1} and 1732 cm^{-1}) and the shift in PVA/thymol's C-OH stretch (944 cm^{-1}), indicated intermolecular interactions, likely hydrogen bonding, within the composite nanofiber structure.

3.3. In Vitro Drug Release Profiles of PVA-Based Nanofibrous Drug Delivery Systems

The in vitro drug release studies revealed distinct release kinetics for the PVA-based nanofibrous systems. All formulations displayed a biphasic release pattern, characterized initially by a slow release phase, followed by a more rapid release phase, culminating in a plateau. The PVA-nystatin combination exhibited the most rapid and substantial release, reaching 95% of the drug payload within 76 hours (Figure 3). The PVA-thymol combination demonstrated a comparable release rate, achieving 86% release within the same timeframe. In contrast, the PVA-nystatin-thymol triple-drug delivery system displayed a slower, more sustained release profile, reaching 84% release after 80 hours.

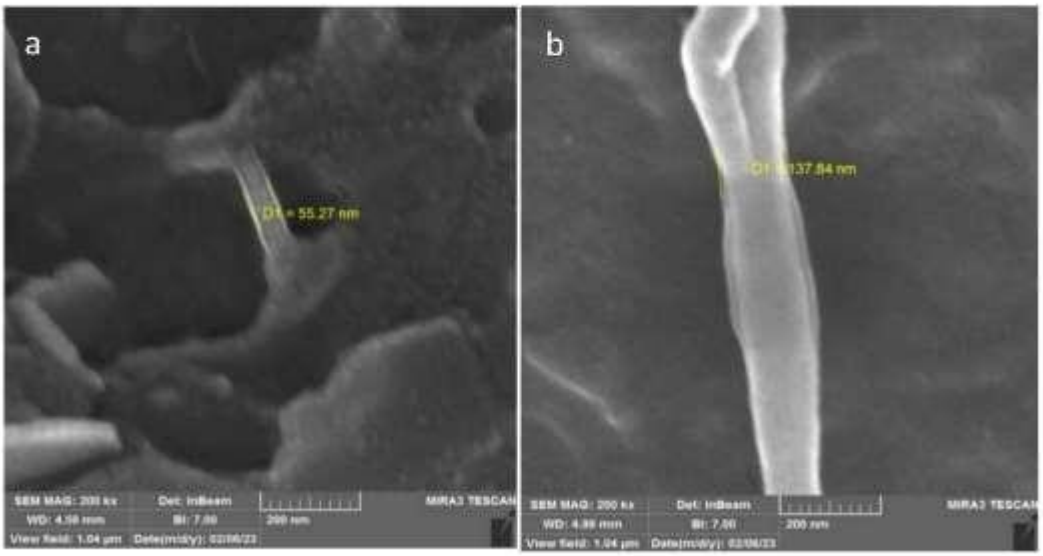

Fig. 1. SEM images of polyvinyl alcohol-nystatin-thymol nanofibers showing smooth and uniform morphology. (A) Broader view with fiber diameter of 55.27 nm. (B) Close-up view with fiber diameter of 137.84 nm. Field of view 1.04 µm, magnification kx200, sample to lens distance 4.59 mm.

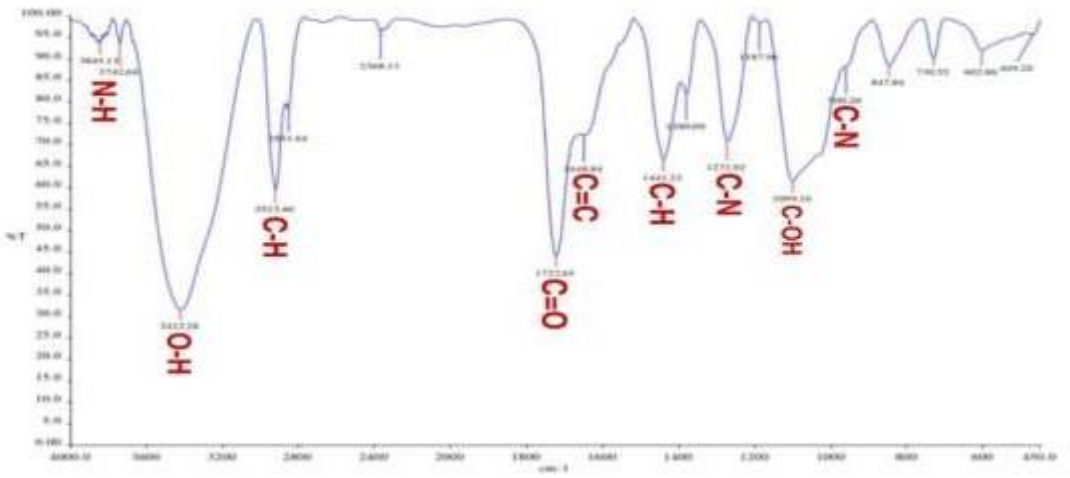

Fig. 2. FT-IR spectrum of PVA-NYS-THY nanofibers. The spectrum reveals the functional groups and the interactions of the compounds. The peaks of O-H, C-H, C=O, C=C, C-N, and C-O bonds are observed. The peak of C=O bond of nystatin splits and the peak of C-O bond of PVA or thymol shifts, indicating complexation and intermolecular forces. The interactions suggest hydrogen bonds between the hydroxyl, carbonyl, and amine groups of PVA, nystatin, and thymol.

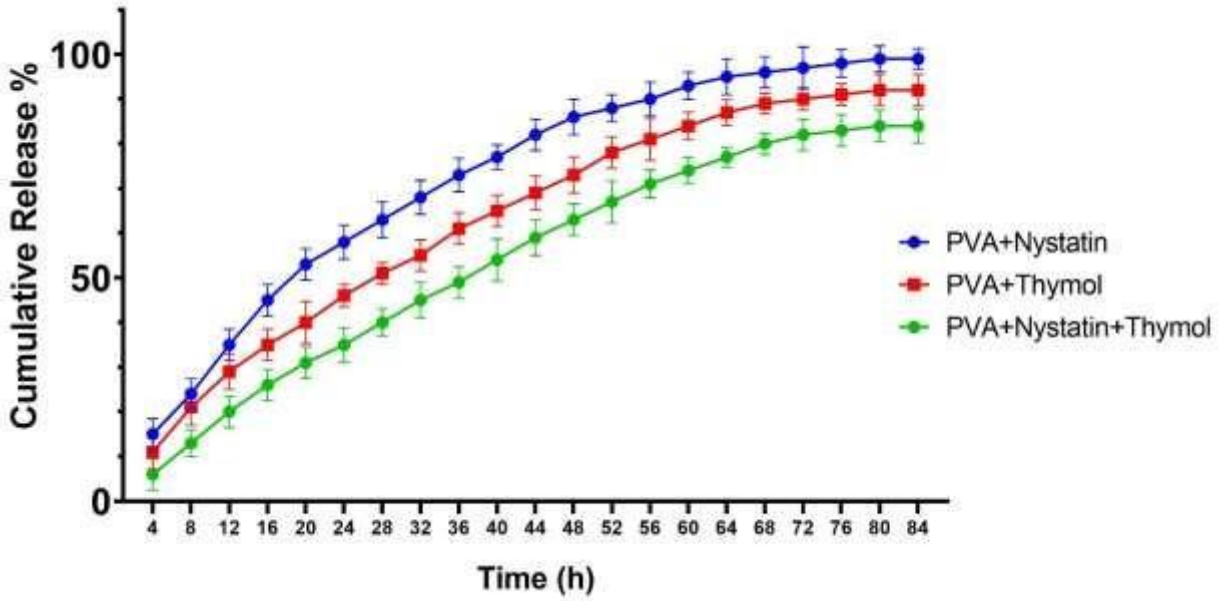

Fig. 3. Drug release profiles of PVA-nystatin, PVA-thymol, and PVA-nystatin-thymol nanofibers. The drug release curves showed a controlled pattern. The PVA-nystatin nanofibers had the highest and fastest drug release, reaching

95% after 76 hours. The PVA-thymol nanofibers had the second highest and fastest drug release, reaching 86% after 76 hours. The PVA-nystatin-thymol nanofibers had the lowest and slowest drug release, reaching 84% after 80 hours.

3.4. Qualitative Antibiogram test results

Qualitative antibiograms revealed that PVA-based nanofibrous scaffolds exhibited antifungal activity against *C. albicans* (control) and *C. glabrata*. Inhibition zones varied across the different formulations (Table 2). Importantly, the PVA-nystatin-thymol composite demonstrated the most potent activity against *C. glabrata*, with inhibition zones ranging from 33 to 37 mm. The PVA-nystatin combination also demonstrated robust activity, exhibiting inhibition zones between 27 and 31 mm. In contrast, the PVA-thymol scaffold displayed the lowest antifungal activity, with zones ranging from 12 to 15 mm.

3.5. MIC, MFC, and FICI results

The antifungal potency of NYS, THY, and PVA, alone and in combination, was assessed against *C. glabrata* by determining MIC, MFC, and FIC indices (Table 3). Results indicated that PVA-based nanofibers exhibited enhanced antifungal activity compared to the individual drugs. Both PVA-NYS and PVA-THY formulations displayed lower MIC and MFC values than their respective free drug counterparts, suggesting that PVA potentiated the antifungal efficacy of NYS and THY. The FIC values for PVA-NYS and PVA-THY (both 0.25) further confirmed this synergistic effect, indicating that the combined action of the drugs with PVA exceeded the additive effect. Importantly, the PVA-NYS-THY nanofibers demonstrated even more pronounced synergy, with a lower FIC value of 0.125.

Table 2. Comparison of the antibacterial activity of three different drug combinations against eight *C. glabrata* isolates. The values represent the diameter of the inhibition zone (in millimeters) measured after 24 hours of incubation.

Isolates	PVA-Nystatin	PVA-Thymol	PVA-Nystatin-Thymol
A1	30 ± 3.1	14 ± 0.9	35 ± 3.4
A2	30 ± 1.4	12 ± 1.7	37 ± 2.7
A3	31 ± 1.8	13 ± 1.1	33 ± 0.8
A4	27 ± 3.5	14 ± 0.8	35 ± 2.6
A5	30 ± 2.7	15 ± 1.3	34 ± 2.5
A6	30 ± 4.2	13 ± 0.9	37 ± 3.1

A7	31 ± 1.5	14 ± 1.2	35 ± 2.2
A8	30 ± 2.6	15 ± 0.6	35 ± 2.3

Table 3. MIC, SubMIC, MFC, and FICI values in different drug groups against *C. glabrata*

Drug formulation	MIC (µg/mL)	SubMIC (µg/mL)	MFC (µg/mL)	FICI
Nystatin	62.5	31.25	125	-
Nystatin-PVA	15.62	7.81	31.25	0.25
Thymol	250	125	500	-
Thymol-PVA	62.5	31.25	125	0.25
Nystatin-Thymol	62.5	31.25	125	-
Nystatin-Thymol-PVA	7.81	3.9	15.62	0.125

3.6. Modulation of *C. glabrata* Virulence Gene Expression by Antifungal Nanofibrous Systems

This study investigated the impact of antifungal agents Nystatin and Thymol, alone and in combination with PVA, on the expression of virulence genes ALS and SAP in *C. glabrata*. Both genes were significantly downregulated in all treatment groups compared to the control. Nystatin alone reduced ALS expression by 51% and SAP by 49%, with further reductions observed when combined with PVA. Thymol alone decreased ALS by 47% and SAP by 42%, also enhanced by PVA addition. The most substantial downregulation was achieved with the combined treatment of Nystatin, Thymol, and PVA, resulting in a 65% reduction in ALS and a 68% reduction in SAP expression (Figure 4).

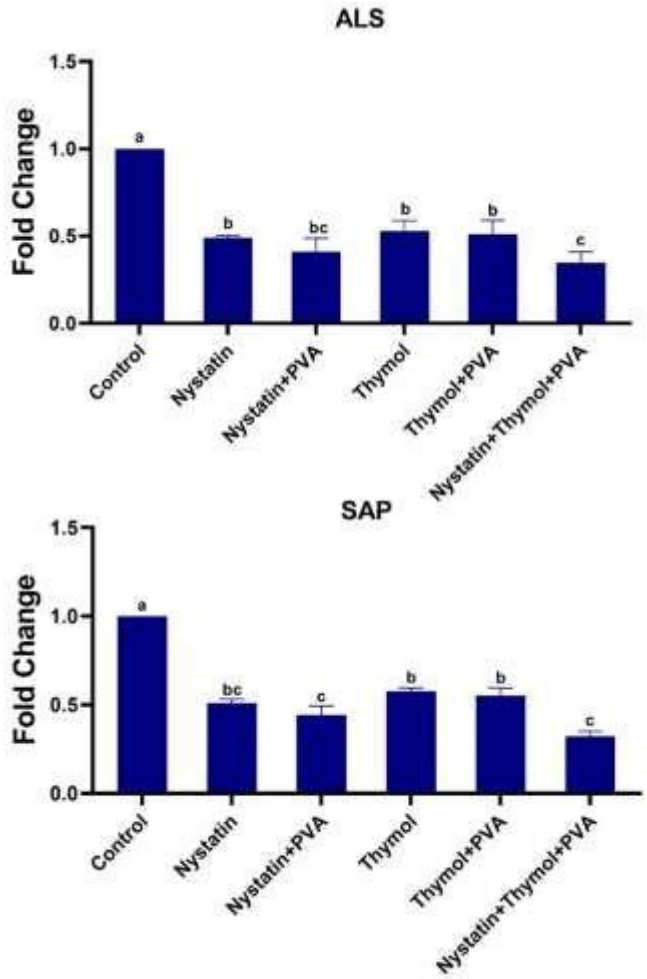

Fig. 4. Expression of *ALS* and *SAP* genes in *C. glabrata* under different antifungal treatments. The expression of *ALS* and *SAP* genes, which encode for agglutinin-like sequence proteins and secreted aspartyl proteinases, respectively, was measured by RT-PCR in *C. glabrata* isolates exposed to various antifungal drugs: nystatin (NYS), thymol (THY), polyvinyl alcohol (PVA), or their combinations. The expression levels were normalized to the control group, which received no treatment. The results showed that the expression of both genes decreased significantly in all drug groups compared to the control group ($P < 0.05$). The control group had the highest expression level of both genes, followed by THY, THY+PVA, and NYS groups, which had similar expression levels. The NYS+PVA and NYS+THY+PVA groups had the lowest expression level of both genes. Means followed by the same letter do not differ significantly by Tukey test.

4. Discussion

In this study, we developed polyvinyl alcohol-nystatin-thymol (PVA-NYS-THY) nanofibers to target *C. glabrata*, a fluconazole-resistant pathogen. Clinical strains of *C. glabrata* were isolated from patient specimens. The nanofibers were characterized using various analytical techniques, and their antifungal efficacy was assessed through MIC, MFC,

and FICI assays. We also investigated *ALS* and *SAP* gene expression, crucial for *C. glabrata* virulence, using PCR and qRT-PCR methods.

Our findings revealed that *C. glabrata* accounted for 13% of the total isolates and 26% of the *Candida* isolates, aligning with previous reports that identify *C. glabrata* as the second most prevalent *Candida* species after *C. albicans* (14). The majority of the *C. glabrata* isolates were obtained from oral swabs (69%), followed by vaginal swabs (23%) and urine samples (8%), reflecting the typical distribution of candidiasis across different anatomical sites (15). Morphological and biochemical analyses confirmed the classical characteristics of *C. glabrata*. Antifungal susceptibility testing showed that all *C. glabrata* isolates were resistant to fluconazole, consistent with the species' propensity for azole resistance, often mediated by efflux pump overexpression and ERG11 mutations (4). However, the isolates were susceptible or semi-susceptible to polyene antifungals, including amphotericin B and nystatin, and exhibited susceptibility to ketoconazole. These findings highlight the need to explore mechanisms driving variable azole responses for better candidiasis treatment strategies.

We synthesized PVA-NYS-THY nanofibers using electrospinning, with polyvinyl alcohol (PVA) as the carrier polymer, and nystatin (NYS) and thymol (THY) as the active antifungal agents. PVA's biodegradability and biocompatibility make it ideal for forming smooth, uniform nanofibers (16). NYS and THY were chosen for their established antifungal properties, low molecular weights, and polarities, facilitating their integration with PVA (7). These agents can form hydrogen bonds with PVA, potentially enhancing the nanofibers' stability and uniformity (16). Formulation optimization ensured defect-free fibers. SEM revealed uniform nanofibers with an average diameter of ~200 nm. Fourier-transform infrared (FT-IR) spectroscopy confirmed the presence of characteristic functional groups and interactions, indicating structural integrity and functional performance of the nanofibers (17). These results demonstrate PVA-NYS-THY nanofibers as a promising platform for antifungal drug delivery.

The controlled release behavior of PVA-NYS-THY nanofibers was monitored, revealing a pattern suitable for sustained drug delivery. The solubility and affinity of NYS and THY for the PVA matrix influenced their release profiles (18). NYS, with higher solubility and lower PVA affinity, exhibited a more rapid initial release, while THY, with moderate solubility and affinity, showed a more sustained release. The combination within the nanofiber matrix resulted in a release profile that combined aspects of both individual drugs, demonstrating the potential for controlled

and prolonged release. These findings suggest the potential of PVA-NYS-THY nanofibers for customizable drug delivery.

The antifungal efficacy of PVA-NYS-THY nanofibers against *C. glabrata* was assessed through inhibition zones, MIC, and MFC measurements. The results demonstrated that antifungal activity correlated with the concentration and composition of NYS and THY, which is related to the drug release kinetics from the nanofiber matrix (19). NYS disrupts the fungal cell membrane by binding to ergosterol, while THY's mechanism of action involves disruption of membrane integrity, binding to ergosterol, and increased membrane permeability, facilitating antifungal entry (9). Resistance mechanisms in *C. glabrata* involve reduced ergosterol for NYS and efflux pump upregulation or enzyme modification for THY (20). PVA-NYS-THY nanofibers exhibited the most potent activity, with the largest inhibition zones and lowest MIC and MFC values. The synergistic effect of NYS and THY, demonstrated by the FICI, enhances the therapeutic potential of this formulation against fluconazole-resistant *C. glabrata*. This synergy is likely due to the combined membrane disruption and other mechanisms of action of the two drugs.

We investigated the presence of *ALS* and *SAP* genes in *C. glabrata* isolates using PCR. These genes encode agglutinin-like sequence (ALS) proteins and secreted aspartyl proteinases (SAP), key virulence factors involved in adhesion and pathogenicity (11). All tested *C. glabrata* isolates (n=8) were positive for both genes, suggesting their consistent co-occurrence and potential role in facilitating invasive infections (21). The co-expression of *ALS* and *SAP* may enhance the organism's ability to colonize host tissues and evade immune defenses, making them important targets for future therapeutic strategies. Further research should investigate the regulation of these genes and their precise roles in antifungal resistance and virulence.

We investigated the effects of NYS and THY, alone and in combination with PVA, on *ALS* and *SAP* gene expression in *C. glabrata* (22). NYS alone reduced *ALS* and *SAP* expression, while THY also decreased the expression of both genes. The combination of NYS and THY with PVA further amplified these effects, with the PVA-NYS-THY combination showing the greatest reduction in both *ALS* and *SAP* expression. This enhanced effect likely results from the combined mechanisms of action of NYS and THY (membrane disruption and oxidative stress, respectively) (20), potentially enhanced by PVA's influence on drug stability and delivery. This downregulation of virulence genes suggests a potential mechanism by which the nanofibers exert their antifungal effect. The downregulation of *ALS* and *SAP* may be linked to disruption of regulatory pathways involving transcriptional regulators like Rim101p, Hap43p,

and Efg1p (23). NYS and THY may influence these regulators through mechanisms such as altering ambient pH (activating Rim101p, repressing *ALS*) or generating reactive oxygen species (ROS) (activating Hap43p, repressing *SAP*) (24). Disruption of ergosterol biosynthesis can also affect regulators like Efg1p (25). Further studies are needed to elucidate the precise molecular mechanisms involved. The enhanced downregulation of *ALS* and *SAP* in the PVA-NYS-THY group suggests that combining these agents within the nanofiber formulation can effectively reduce *C. glabrata* virulence.

This study has important implications for future research and clinical practice. It demonstrates electrospinning as a promising technique for developing antifungal formulations that deliver natural agents like NYS and THY in a controlled manner. It also shows that NYS and THY act synergistically against *C. glabrata*, enhancing their antifungal activity. Furthermore, the study reveals that these agents can modulate *ALS* and *SAP* gene expression, potentially reducing *C. glabrata* virulence. Future research should assess biocompatibility and conduct *in vivo* testing to evaluate the clinical potential of these nanofibers.

Acknowledgment

The authors would like to thank the staff of the Islamic Azad University (IAU) laboratory in North Tehran Branch (Iran) for their effective cooperation.

Authors' contribution

Study concept and design: M.L. and M.B. Analysis and interpretation of data: R.A. and M.L. Drafting of the manuscript: R.A. Critical revision of the manuscript for important intellectual content: M.L. and M.B. Statistical analysis: R.A. and M.L.

Ethical Approval

The authors confirm that this study was approved by the research ethics committee of Research Ethics Committees of Islamic Azad University (RECIAU no: 1401.0445) and certify that this study was performed in accordance with the ethical standards as laid down in the 1964 Declaration of Helsinki and its later amendments or comparable ethical standards.

Conflict of Interest

The authors declare that they have no conflict of interest.

Data Availability

The data that support the findings of this study are available on request from the corresponding author.

References

1. Hassan Y, Chew SY, Than LTL. *Candida glabrata*: Pathogenicity and Resistance Mechanisms for Adaptation and Survival. J Fungi (Basel). 2021;7(8).
2. Sachivkina N, Podoprigora I, Bokov D. Morphological characteristics of *Candida albicans*, Candida krusei, Candida guilliermondii, and *Candida glabrata* biofilms, and response to farnesol. Vet World. 2021;14(6):1608-14.
3. Szymański M, Chmielewska S, Czyżewska U, Malinowska M, Tylicki A. Echinocandins - structure, mechanism of action and use in antifungal therapy. J Enzyme Inhib Med Chem. 2022;37(1):876-94.
4. Esfahani A, Omran AN, Salehi Z, Shams-Ghahfarokhi M, Ghane M, Eybpoosh S, et al. Molecular epidemiology, antifungal susceptibility, and ERG11 gene mutation of Candida species isolated from vulvovaginal candidiasis: Comparison between recurrent and non-recurrent infections. Microb Pathog. 2022;170:105696.
5. Aderibigbe BA. Nanotherapeutics for the delivery of antifungal drugs. Ther Deliv. 2024;15(1):55-76.
6. Han WH, Wang QY, Kang YY, Shi LR, Long Y, Zhou X, et al. Cross-linking electrospinning. Nanoscale. 2023;15(38):15513-51.
7. Sousa F, Nascimento C, Ferreira D, Reis S, Costa P. Reviving the interest in the versatile drug nystatin: A multitude of strategies to increase its potential as an effective and safe antifungal agent. Adv Drug Deliv Rev. 2023;199:114969.
8. Rai A, Misra SR, Panda S, Sokolowski G, Mishra L, Das R, et al. Nystatin Effectiveness in Oral Candidiasis Treatment: A Systematic Review & Meta-Analysis of Clinical Trials. Life (Basel). 2022;12(11).
9. Salehi B, Mishra AP, Shukla I, Sharifi-Rad M, Contreras MDM, Segura-Carretero A, et al. Thymol, thyme, and other plant sources: Health and potential uses. Phytother Res. 2018;32(9):1688-706.
10. de Castro RD, de Souza TM, Bezerra LM, Ferreira GL, Costa EM, Cavalcanti AL. Antifungal activity and mode of action of thymol and its synergism with nystatin against Candida species involved with infections in the oral cavity: an in vitro study. BMC Complement Altern Med. 2015;15:417.
11. Bonfim-Mendonça PdS, Tobaldini-Valério FK, Capoci IR, Faria DR, Sakita KM, Arita GS, et al. Different expression levels of ALS and SAP genes contribute to recurrent vulvovaginal candidiasis by *Candida albicans*. Future Microbiol. 2021;16(4):211-9.
12. Aduba Jr DC, An S-S, Selders GS, Yeudall WA, Bowlin GL, Kitten T, et al. Electrospun gelatin–arabinoxylan ferulate composite fibers for diabetic chronic wound dressing application. International Journal of Polymeric Materials and Polymeric Biomaterials. 2019;68(11):660-8.
13. Alves CT, Wei XQ, Silva S, Azeredo J, Henriques M, Williams DW. *Candida albicans* promotes invasion and colonisation of *Candida glabrata* in a reconstituted human vaginal epithelium. J Infect. 2014;69(4):396-407.
14. Aghili SR, Abastabar M, Soleimani A, Haghani I, Azizi S. High prevalence of asymptomatic nosocomial candiduria due to *Candida glabrata* among hospitalized patients with heart failure: a matter of some concern? Curr Med Mycol. 2020;6(4):1-8.
15. Morales-López SE, Taverna CG, Bosco-Borgeat ME, Maldonado I, Vivot W, Szusz W, et al. *Candida glabrata* species complex prevalence and antifungal susceptibility testing in a culture collection: First description of Candida nivariensis in Argentina. Mycopathologia. 2016;181(11-12):871-8.
16. Morais MS, Bonfim DPF, Aguiar ML, Oliveira WP. Electrospun Poly (Vinyl Alcohol) Nanofibrous Mat Loaded with Green Propolis Extract, Chitosan and Nystatin as an Innovative Wound Dressing Material. J Pharm Innov. 2022:1-15.
17. Mohammadi G, Shakeri A, Fattahi A, Mohammadi P, Mikaeili A, Aliabadi A, et al. Preparation, Physicochemical Characterization and Anti-fungal Evaluation of Nystatin-Loaded PLGA-Glucosamine Nanoparticles. Pharm Res. 2017;34(2):301-9.
18. Czibulya Z, Csík A, Tóth F, Pál P, Csarnovics I, Zelkó R, et al. The Effect of the PVA/Chitosan/Citric Acid Ratio on the Hydrophilicity of Electrospun Nanofiber Meshes. Polymers (Basel). 2021;13(20).

19. Balusamy B, Celebioglu A, Senthamizhan A, Uyar T. Progress in the design and development of "fast-dissolving" electrospun nanofibers based drug delivery systems - A systematic review. Journal of Controlled Release. 2020;326:482-509.
20. Sahoo CR, Paidesetty SK, Padhy RN. The recent development of thymol derivative as a promising pharmacological scaffold. Drug Dev Res. 2021;82(8):1079-95.
21. Gabaldón T, Gómez-Molero E, Bader O. Molecular Typing of *Candida glabrata*. Mycopathologia. 2020;185(5):755-64.
22. Yu S, Li W, Liu X, Che J, Wu Y, Lu J. Distinct expression levels of ALS, LIP, and SAP genes in Candida tropicalis with diverse virulent activities. Front Microbiol. 2016;7:1175.
23. Naglik JR, Challacombe SJ, Hube B. *Candida albicans* secreted aspartyl proteinases in virulence and pathogenesis. Microbiol Mol Biol Rev. 2003;67(3):400-28, table of contents.
24. Puri S, Kumar R, Rojas IG, Salvatori O, Edgerton M. Iron Chelator Deferasirox Reduces *Candida albicans* Invasion of Oral Epithelial Cells and Infection Levels in Murine Oropharyngeal Candidiasis. Antimicrobial Agents and Chemotherapy. 2019;63(4):10.1128/aac.02152-18.
25. Jordão CC, Klein MI, Carmello JC, Dias LM, Pavarina AC. Consecutive treatments with photodynamic therapy and nystatin altered the expression of virulence and ergosterol biosynthesis genes of a fluconazole-resistant *Candida albicans* in vivo. Photodiagnosis Photodyn Ther. 2021;33:102155.